Electronic Supplementary Material (ESI) for Inorganic Chemistry Frontiers.

Supporting Information

Iron(II) pillared-layer Supramolecular Frameworks via “kagomé dual” (kgd) Supramolecular Tessellations

Shufang Xue, Liang Wang, Anil D. Naik, Julianna Oláh, Koen Robeyns, Aurelian Rotaru, Yunnan Guo* and Yann Garcia*

yann.garcia@uclouvain.be

1. Instrumentation

Diffuse-reflectance UV-Vis-spectra (DRS) were recorded using a Shimadzu Perkin Elmer Lambda 9 UV/vis/NIR spectrophotometer. $BaSO_4$ powder was used as the reference (100% reflectance).

Powder X-ray Diffraction (PXRD) experiments were carried out on a D8 Advanced diffractometer from Bruker. The diffractogram was recorded using CuKα radiation (λ = 1.5406 Å) and a linkeye XE-T detector (Bruker) in the 5–50° (2θ) range with an increment of 0.00151° and an integration time of 0.15 s.

Magnetic susceptibility measurements for all the complexes were carried out on a MPMS3 SQUID magnetometer (Quantum Design Inc.) in the DC mode, under a DC magnetic field of 1000 Oe, with a temperature rate of 2 K min^{-1}. Magnetic data were corrected for both sample holder complex diamagnetic contributions.

^{57}Fe Mössbauer spectra were recorded at room temperature in the transmission geometry mode with a constant acceleration mode conventional Wissel Mössbauer spectrometer equipped with a $^{57}Co(Rh)$ radioactive source, a Reuter Stokes proportional counter detector and a CMCA-550 multichannel analyzer. All isomer shifts in Mössbauer spectra are given with respect to α-Fe.

TGA experiments were performed in $N_{2(g)}$ (100 mL min^{-1}) at a heating rate of 10 K min^{-1} from 298 to 873 K using a Mettler Toledo TGA/SDTA 851e analyzer.

2. Single crystal X-ray analyses

X-ray intensity data were collected at 150 K on a MAR345 image plate using MoKα radiation (λ = 0.71073Å). The crystals were selected, mounted in inert oil and transferred to the cold gas stream for flash cooling. Data were integrated by Crysalis (Agilent Technologies (2012). Agilent Technologies UK Ltd., Oxford, UK, Xcalibur/SuperNova CCD system, CrysAlisPro Software system, Version 1.171.36.21.). Absorption correction was applied using the integrated multi-scan absorption algorithm. The structures were solved by direct methods (SHELXS) and refined by full-matrix least-squares on $|F^2|$ using SHELXL97 (G. M. Sheldrick, *Acta Cryst*. 2008, **A64**, 112-122.). All nonhydrogen atoms were refined with anisotropic temperature factors. Aromatic H atoms were placed at calculated positions and ride on the parent atom. For the coordinated H2O and lattice water molecules, H atoms were found in the Fourier difference map, refined to idealized geometry and refined as a rigid group which was allowed to rotate around the oxygen atom. H-atoms were refined isotropically with temperature factors set at 1.2 times the Ueq of the parent atoms. The crystal was found to be twinned and the twinrotmat procedure in Platon (A. L. Spek, *Acta Cryst*. 2009, **D65**, 148-155.) was used to generate a twin-corrected intensity file (refined twin fraction: 0.31415). CCDC 2031041 and 2031042 contain the supplementary crystallographic data for this paper. These data can be obtained free of charge from CCDC via www.ccdc.cam.ac.uk/data_request/cif.

Table S1. Crystal data and structure refinement details for **Fe-w0**, **Fe-w4** and **Fe-w5**.

Compound reference	**Fe-w0**	**Fe-w4** [1]	**Fe-w5**
Molecular formula	$C_6H_{12}FeN_{14}O_4$	$C_6H_{20}FeN_{14}O_8$	$C_6H_{22}FeN_{14}O_9$
Formula weight, g/mol	400.15	472.21	490.23
T/K	150(2)	120	150(2)
λ/Å	0.71073	0.71073	0.71073
Crystal system	Monoclinic	Triclinic	Monoclinic
Space group	*C*2/*c*	*P***Error!**	*P*21/*n*
a/Å	6.0747(3)	6.5493(11)	6.8715(7)
b/Å	11.1004(4)	7.5664(19)	12.8192(16)
c/Å	21.2369(9)	10.749(3)	22.670(2)
α/°	90.00	104.83(2)	90
β/°	98.218(4)	94.614(18)	96.870(9)
γ/°	90.00	111.186(19)	90
V/Å^3	1417.34(10)	471.21(19)	1982.6(4)
Z	4	1	4
ρ_{calcd}/g·cm^{-3}	1.875	1.664	1.642
μ/mm^{-1}	1.121	0.871	1.434
F(000)	816	244	384
*Crystal size/*mm^{-1}	0.35 x 0.25 x 0.25	0.16 x 0.13 x 0.13	0.25 x 0.05 x 0.05
θ range for data collection/°	3.67 to 25.74	-	3.146 to 24.107
Index ranges	$-7 \le h \le 7$ $-13 \le k \le 13$ $-6 \le l \le 25$	-	$-7 \le h \le 7$ $-14 \le k \le 14$ $-4 \le l \le 25$
No. of independent reflections	1337	-	3122
R_{int}	0.0138	-	0.0911
Final R_1 values ($I > 2\sigma(I)$)	0.0237	-	0.0764
Final $wR(F^2)$ values (all data)	0.0617	-	0.1734
Goodness of fit on F^2	1.143	-	1.045
Largest diff. peak and hole/e Å^{-3}	0.415 and -0.327	-	1.451 and -0.429

Table S2. Selected bond distances (Å) and angles (°) in **Fe-w0** and **Fe-w5**.

Fe-w0					
Fe1-O2	2.0875(18)	Fe1-N4	2.1897(19)	Fe1-O3	2.1972(17)
O2-Fe1-O2#1	87.04(10)	N4-Fe1-N4#1	173.41(11)	O2-Fe1-O3#1	92.87(6)
O2-Fe1-N4	92.81(7)	O2-Fe1-O3	179.78(7)	N4-Fe1-O3#1	88.23(7)
O2#1-Fe1-N4	91.97(7)	N4-Fe1-O3	86.99(7)	O3-Fe1-O3#1	87.22(9)
Symmetry code #1: - *x*, *y*, -*z* + 1/2					
Fe-w5					
Fe1-O5	2.081(6)	Fe1-O2	2.106(6)	Fe1-N21	2.174(9)
Fe1-O3	2.093(6)	Fe1-O4	2.138(7)	Fe1-N11	2.185(8)
O5-Fe1-O3	174.5(3)	O2-Fe1-O4	172.9(3)	O5-Fe1-N11	86.8(3)
O5-Fe1-O2	84.3(3)	O5-Fe1-N21	91.7(3)	O3-Fe1-N11	88.2(3)
O3-Fe1-O2	94.0(3)	O3-Fe1-N21	93.5(3)	O2-Fe1-N11	91.4(3)
O5-Fe1-O4	88.6(3)	O2-Fe1-N21	88.4(3)	O4-Fe1-N11	87.8(3)
O3-Fe1-O4	2.081(6)	O4-Fe1-N21	2.106(6)	N21-Fe1-N11	178.5(3)

3. Supramolecular analyses

Table S3. Geometrical parameters of the supramolecular interactions in the **Fe-w0**, **Fe-w4** and **Fe-w5**. The color shading is corresponding to interactions depicted in the figures of supramolecular structure.

D-H···A	H···A	D···A	D-H···A (°)	Symmetry code
Fe-w0				
HB of triangular tiling in Figure 4				
O2-H2A···O3	2.05	2.881(2)	172	-1/2+x,-1/2+y,z
O3-H3B···N5	2.08	2.858(3)	153	1-x, y, 1/2-z
HB 2D to 3D supramolecular structure (Figure 5)				
O2-H2B···N12	1.91	2.744(3)	173	-1/2-x, 1/2-y, -z
O3-H3A···N11	1.93	2.766(3)	170	x, 1-y, 1/2+z
Fe-w4				
HB of rhombille tiling (Figure 6b, c)				
O2-H2A···O14	1.85	2.685(7)	170	-1+x,y,z
O3-H3A···O14	1.86	2.696(7)	177	1-x,1-y,2-z
O14-H14B···N5	2.08	2.813(7)	145	1-x,-y,2-z
HB pillaring the rhombille tiling to SF (Figure 8)				
O3-H3B···N11	2.05	2.873(7)	165	-x,-y,1-z
O14-H14A···N12	2.00	2.799(7)	160	1-x,-y,1-z
HB of encapsulated H_2O15 Figure S 4)				
O2-H2B···O15	1.90	2.736(6)	174	1-x,1-y,2-z
O15-H15A···N10	2.23	2.991(8)	151	1-x,-y,1-z
O15-H15B···N13	2.10	2.904(7)	161	1-x,1-y,1-z
Fe-w5				
HB for rhombille tiling (Figure 7b, c)				
O2-H2B···O31	1.87	2.705(10)	175	1/2-x, 1/2+y, 3/2-z
O3-H3B···O31	1.87	2.694(10)	168	3/2-x, 1/2+y, 3/2-z
O31-H31A···N22	1.97	2.816(12)	174	
O4-H4A···O32	1.91	2.708(10)	161	
O5-H5A···O32	1.86	2.663(11)	161	-1+x, y, z
O32-H32B···N12	2.03	2.831(11)	159	3/2-x,-1/2+y,3/2-z
HB pillaring the rhombille tiling to SF (Figure 8)				
O31-H31B···N28	2.04	2.820(12)	156	1-x, 1-y, 1-z
O32-H32A···N18	2.04	2.877(11)	177	1/2+x, 3/2-y, -1/2+z

*HB of encapsulated lattice waters (O33, O34 and O35) (*Figure S 5a*)*				
O2-H2A···O35	1.95	2.756(10)	161	
O3-H3A···O33	1.91	2.741(10)	171	
O5-H5B···O35	1.95	2.766(12)	162	1/2-x,-1/2+y,3/2-z
O33-H33B···N19	1.96	2.775(12)	167	1/2+x, 3/2-y, -1/2+z
O34-H34A···N30	2.12	2.896(12)	153	
O34-H34B···N20	2.08	2.901(12)	168	1/2-x, 1/2+y, 3/2-z
*HB of water channel between H_2O33, H_2O34 and H_2O35 (*Figure S 5b*)*				
O33-H33A···O34	2.43	3.076(11)	134	
O35-H35A···O34	1.84	2.687(10)	171	
O35-H35B···O33	2.00	2.806(11)	159	-1+x, y, z

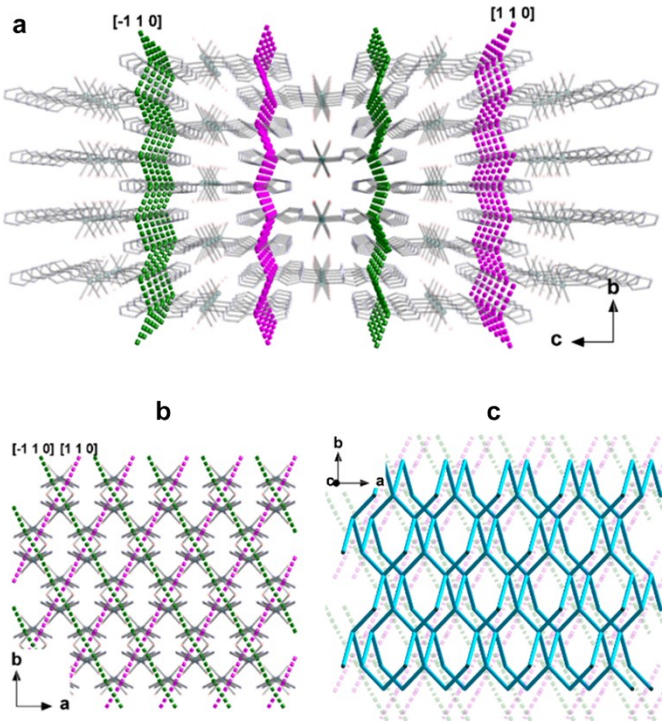

Figure S1. View along (a) [1 0 0] and (b) [0 0 1] direction of the π···π stacking interactions present between adjacent **trz-tet** ligands in **Fe-w0**. The violet and green dashed lines have been added to guide the eye. (c) 3D diamond topology of π-π stacking network abstracted by being the mononuclear unit as a four-connected node.

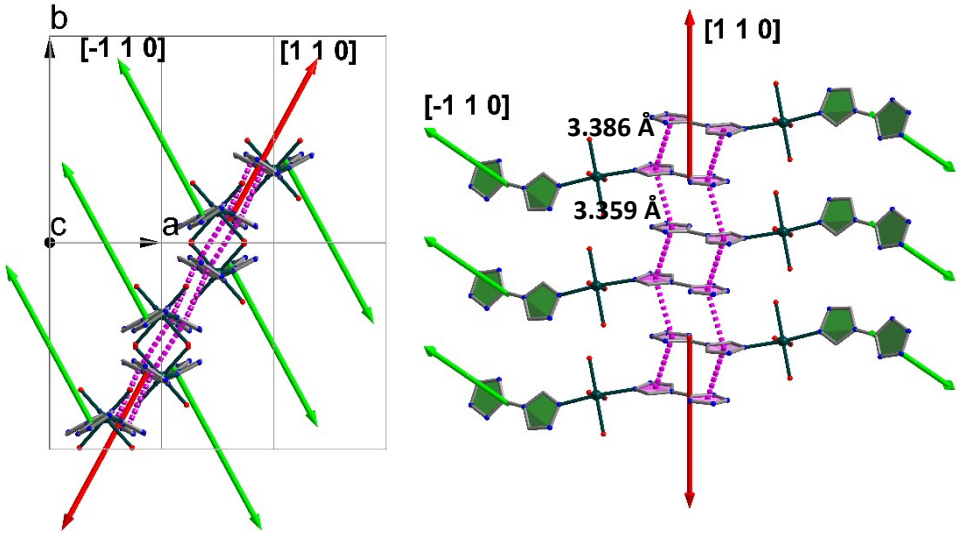

Figure S2. π-π stacking interactions between **trz-tet** ligand along different directions of [1 1 0] and [-1 1 0] in **Fe-w0**.

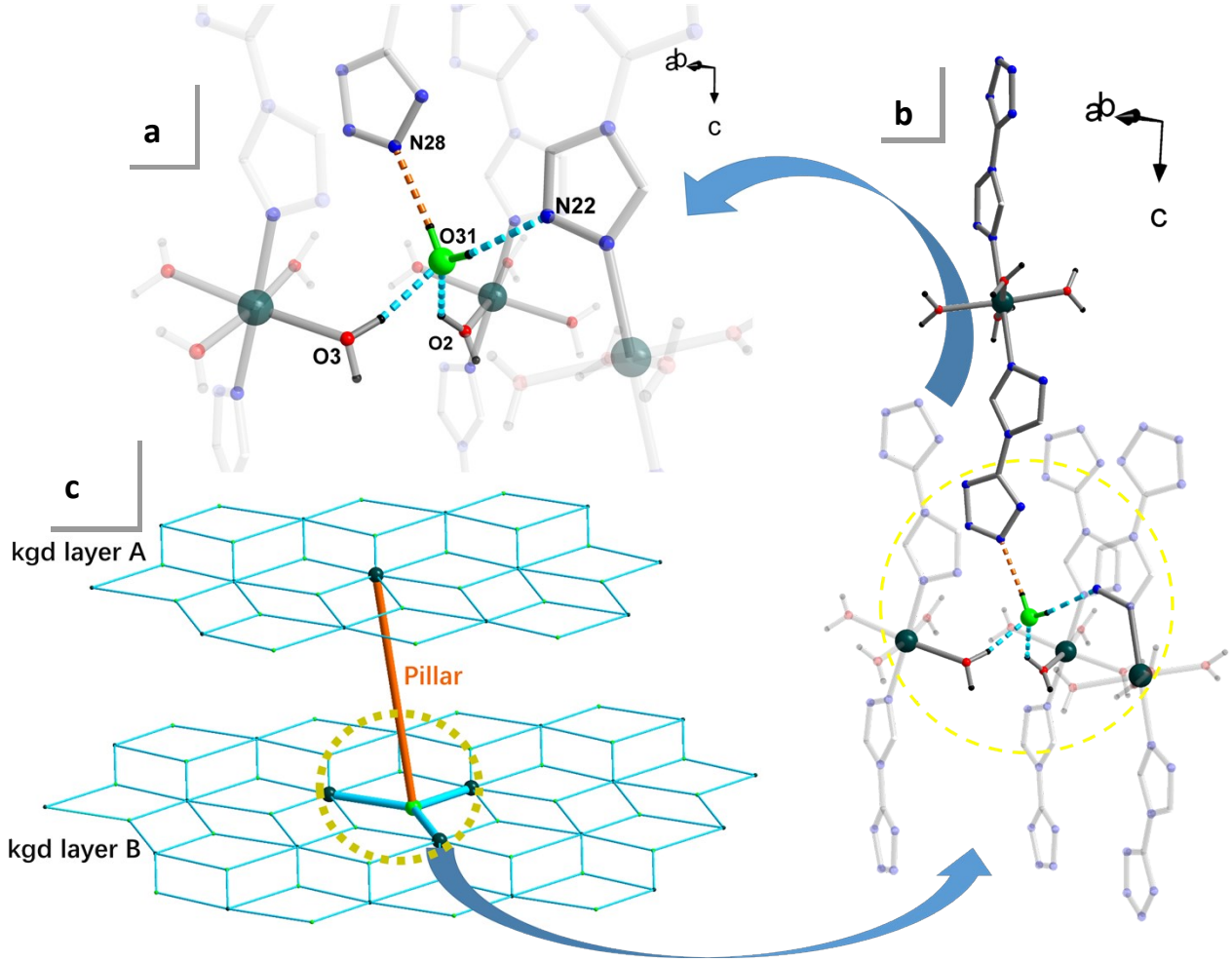

Figure S3. Detailed presentation of pillared-layer SF in **Fe-w5**. (a) and (b) Take H_2O31 as an example, showing AADD manner to connecting four adjacent Fe^{II} molecules. (c) 2-periodic nets within edge-transitive **kgd** layers.

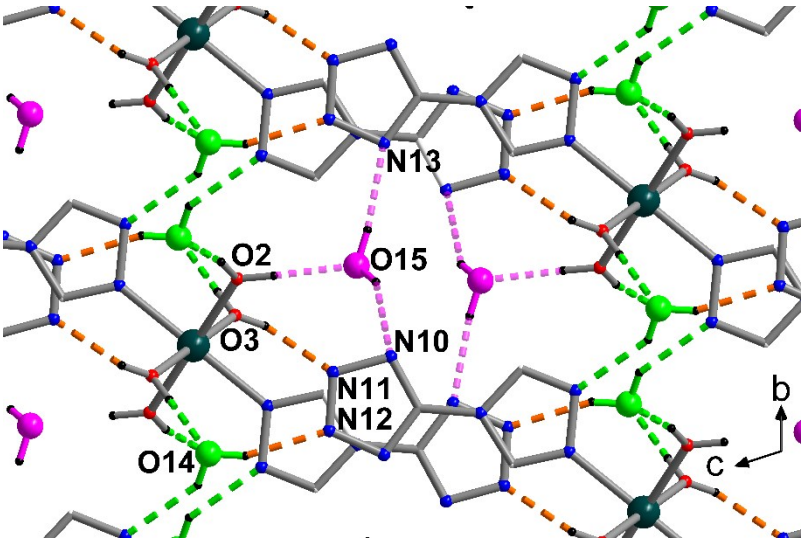

Figure S4. HBs of encapsulated H2O15 in SF **Fe-w4**.

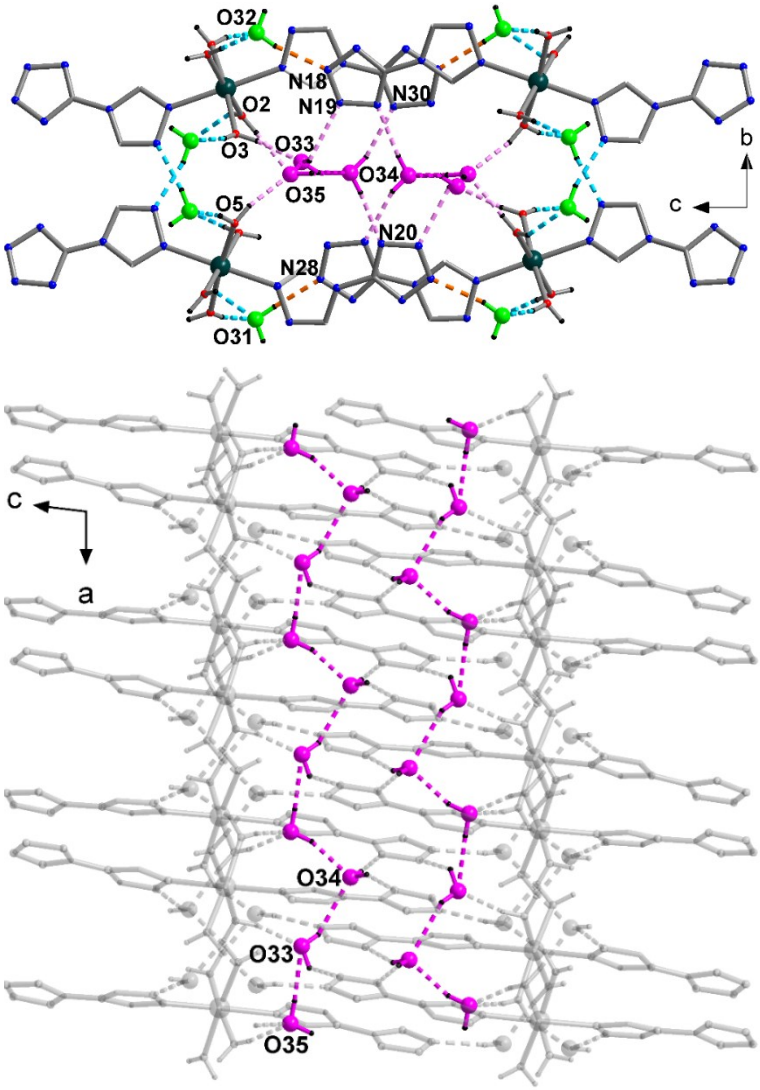

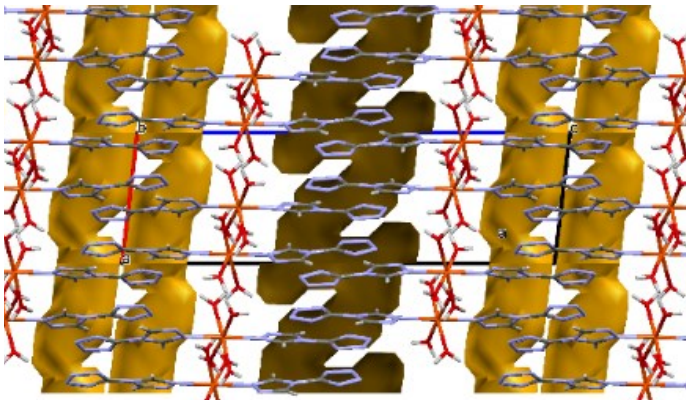

Figure S5. (a) and (b) HBs of 1D water channels in **Fe-w5**. (c) The void (water) space was estimated using a 1.2 Å probe radius and a grid spacing of approx. 0.15 Å, using the voids tool in Mercury software.

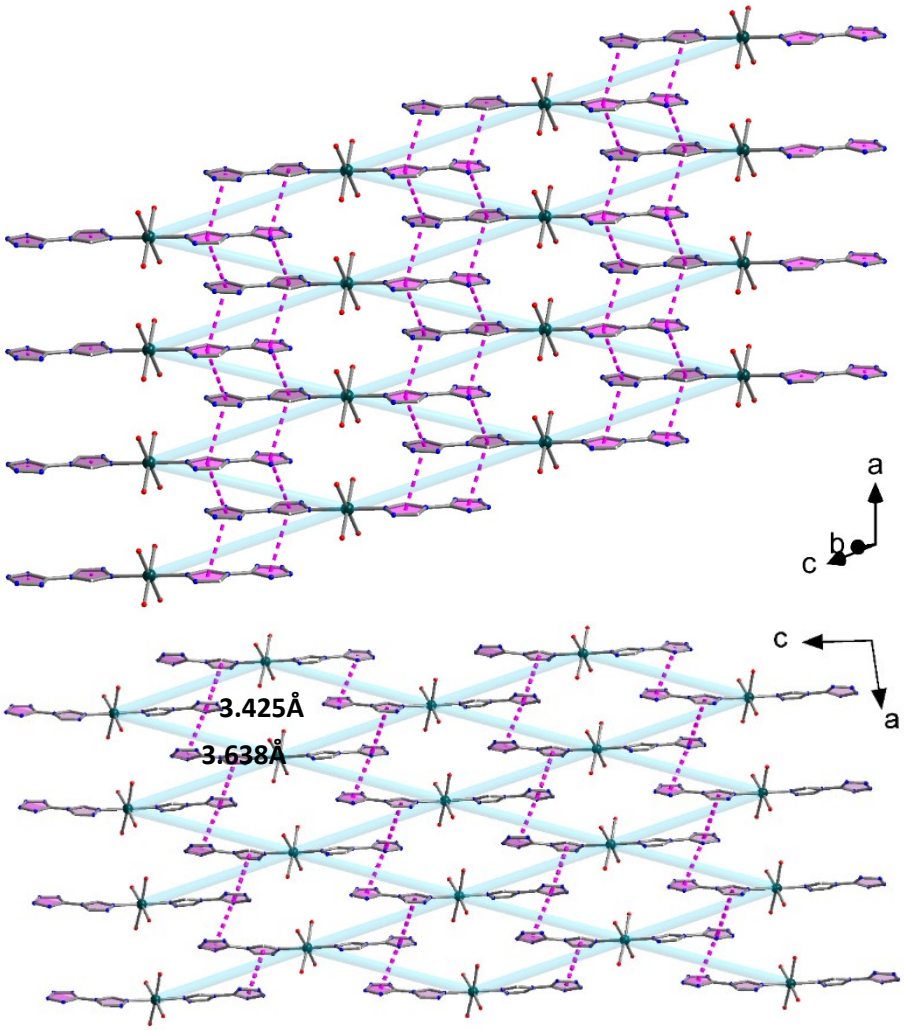

Figure S6. $\pi\cdots\pi$ interactions in **Fe-w4** (top) and **Fe-w5** (bottom).

4. Optical sensing properties and crystal field analyses

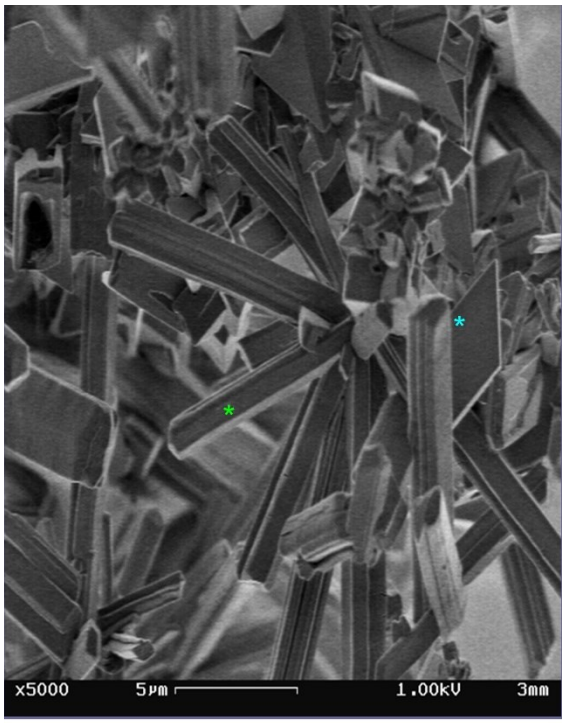

(a)

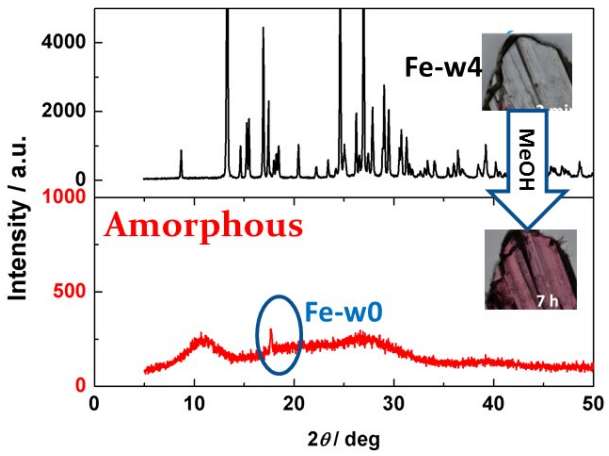

(b)

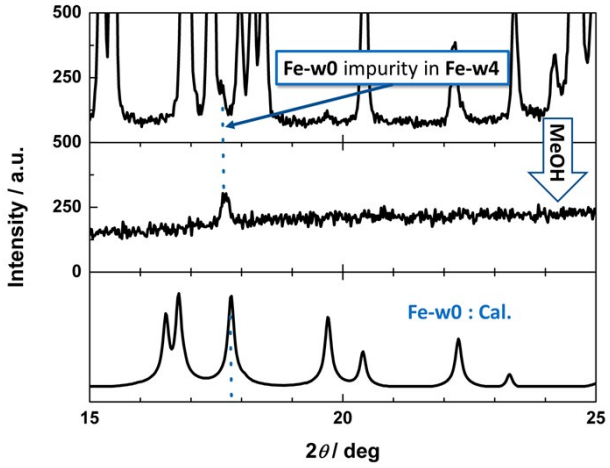

(c)

Figure S7. Fe-w0 as the impurity of **Fe-w4**. (a) SEM image showing both crystals of **Fe-w4** (rods, marked with a green star) and **Fe-w0** (parallelograms, marked with a blue star) ; XRPD diffraction pattern before and after MeOH diffusion: from 5 to 50° (b) and from 15 to 25° (c).

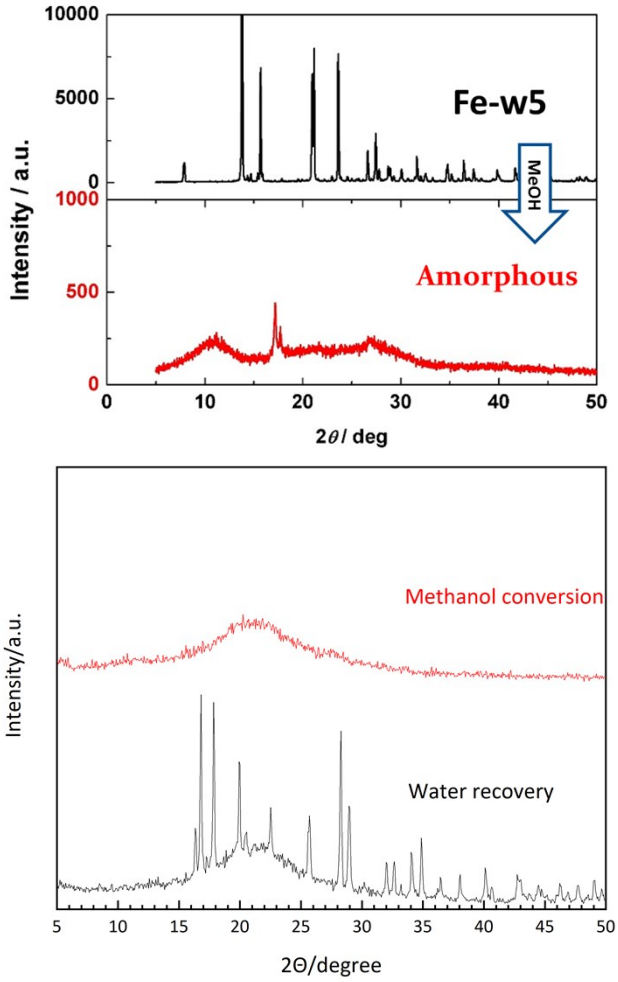

Figure S8 (top) PXRD of **Fe-w5** before and after MeOH diffusion leading to an amorphous phase. (bottom) The regenerated phase by exposure of water recovers a crystalline state.

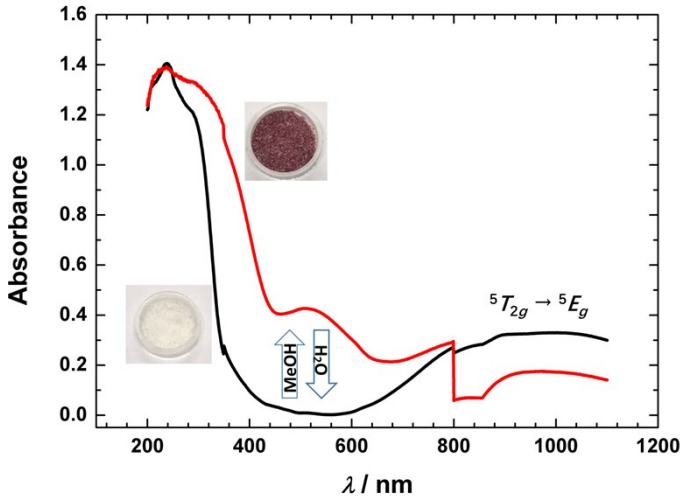

Figure S9. Diffuse-reflectance spectroscopy of reversible and bidirectional colorimetric sensing developed from **Fe-w5** under MeOH or H_2O for sensing or regeneration, respectively.

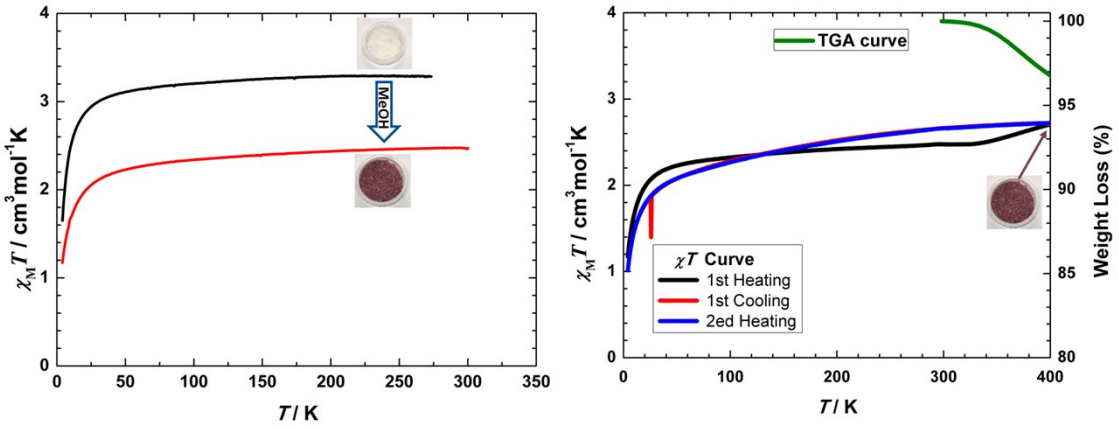

Figure S10. Thermal variation of $\chi_M T$ for **Fe-w5** before and after MeOH diffusion. Before and after sensing of MeOH, the sample shows a paramagnetic state with a constant $\chi_M T$ value as the temperature decreases, with a drop at lowest temperatures due to zero field splitting. The $\chi_M T$ value change about 25% from 3.28 to 2.47 $cm^3mol^{-1}K$ at r.t. after MeOH sensing, which is in agreement with 26% of LS Fe^{II} ions from Mössbauer measurement (See Fig. 11). The impact of the release of MeOH on the magnetic properties was also investigated and compared to weight derived from TGA. The $\chi_M T$ value was found to increase slightly as the MeOH is removed. Such an increase of $\chi_M T$ value did not reflect any SCO properties as shown in the next cycles measurements.

Determination of crystal field splitting energy *Δ*

For a d^6 Fe^{II}(HS) in O_h field, the energy of the transition $^5T_{2g} \rightarrow {}^5E_g$ gives the value of Δ directly, can be extracted from Figure S 9. In other words, the lowest energy absorption band in d^6 HS complexes is equal to the crystal field splitting energy. The $(t_{2g})^4(e_g)^2$ electronic configuration of HS Fe^{II} in octahedral field is bound to undergo a slight Jahn-Teller distortion. The transition from $^5T_{2g}$ to the split components of the ^5E_g level ($^5B_{1g}$ and $^5A_{1g}$) are splitted by an energy difference of around 1000 cm^{-1}. This contributes to the broadening of the band (Figure S 9).

For d^6 Fe^{II}(LS), Δ may not correspond directly to a transition energy. From the Tanabe-Sugano diagram, it can clearly be seen that the spin-allowed *d-d* transitions in LS d^6 Fe^{II} are $^1A_{1g} \rightarrow {}^1T_{1g}$ and $^1A_{1g} \rightarrow {}^1T_{2g}$. In the UV-visible absorption spectra subtracted between **Fe-w5** before and after sensing with MeOH, two bands are observed; one band with maxima at 27700 cm^{-1} and another at 19417 cm^{-1}. Therefore, Δ and B (Racah parameter) can be fixed at 21325 cm^{-1} and 625 cm^{-1}.

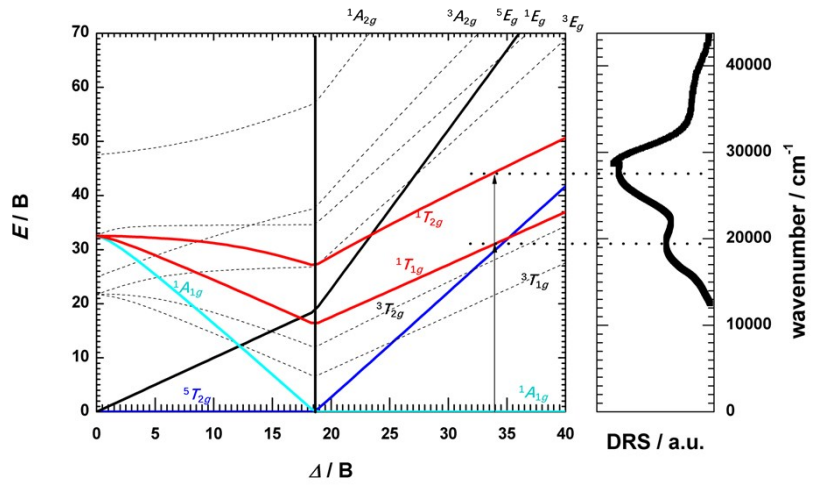

Figure S11. Tanabe-Sugano diagram of d^6 Fe^{II} corresponding the calculation of LS in pink form (**Fe-w5** after sensing with MeOH).

Determination of the Tetragonal distortion based on temperature dependent Mossbauer spectrum

In a iron(II) HS system, it is well know that a large quadrupole splitting reflects that the d^6 configuration with low electric field gradient (EFG) at the nucleus is splitted by a distortion to produce a high EFG situation. Therefore, ΔE_Q is very sensitive as a detector of small distortions. In **Fe-w5**, t_{2g} orbitals was splitted by the distortion from a Jahn-Teller effect. Considering a tetragonal distortion due to the *trans*-FeN_2O_4 configuration, this would produce the EFG tensor of V_{zz} component being $+(4/7)(r^{-3})_{3d}$ (the EFG's for the d_{xy}, d_{xz} and d_{yz} states are $+(4/7)(r^{-3})_{3d}$, $-(2/7)(r^{-3})_{3d}$ and $-(2/7)(r^{-3})_{3d}$, respectively[2], see Figure S 12).

The relation between EFG of V_{zz} and temperature for octahedral ions with tetragonal distortion is given by:[1]

$$V_{zz} = (1-R)(V_{ZZ})_{(CF)} + (1-\gamma_\infty)(V_{ZZ})_{(L)}, \text{ in which } (V_{zz})_{(CF)} = \frac{4}{7}\left(e\left\langle r^{-3}\right\rangle_d\right)\frac{1-\exp\left(\frac{-\varepsilon}{k_BT}\right)}{1+2\exp\left(\frac{-\varepsilon}{k_BT}\right)}$$

$(1-R)$ and $(1-\gamma_\infty)$ are the Sternheimer corrections.[3] In this equation, ε is the value of tetragonal splitting, which determines the distribution of (↓) electron between e_g and b_{2g} (Figure S12). The term $(V_{zz})_{(L)}$ arises from charges on the ligands and distant atoms and will in general be smaller than the first term $(V_{zz})_{(CF)}$ which arises from crystal field on the central ion, particularly, in a Fe^{II} HS system, where EFG is dominated by $(V_{zz})_{(CF)}$.[4]

	d_{xy}	d_{xz}	d_{yz}	d_{x2-y2}	d_{z2}
$\frac{(V_{ZZ})_{CF}}{e<r^{-3}>}$	+4/7	-2/7	-2/7	+4/7	-4/7

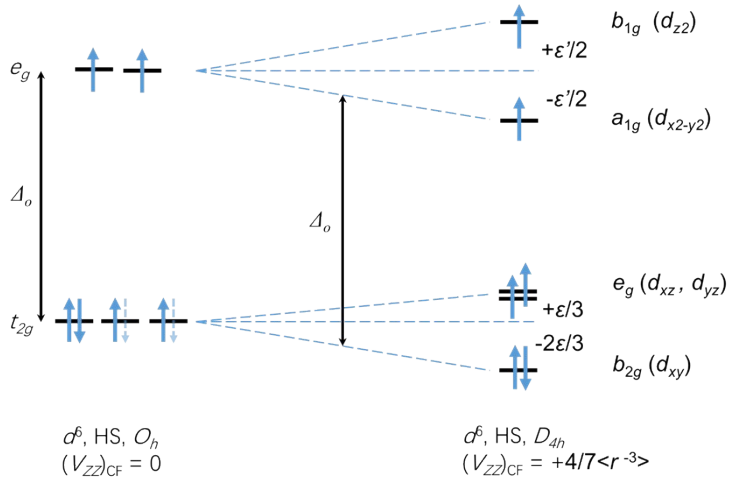

Figure S12. t_{2g} orbitals was splitted by the distortion from Jahn-Teller effect, with EFG tensor of V_{zz} component.

Therefore, the relation between the quadrupole splitting ΔE_Q and temperature may be found by adapting the methods in reference [5], by neglecting the effect of $(V_{zz})_{(L)}$:

$$\Delta E_Q = \frac{1}{2} eQ(V_{zz})_{(CF)} \propto \frac{1-\exp\left(\frac{-\varepsilon}{k_B T}\right)}{1+2\exp\left(\frac{-\varepsilon}{k_B T}\right)}$$

where eQ is the electric quadrupole moment of the 14.4-keV state of ^{57}Fe. The magnitude of ε was determined by computation based on $\Delta E_Q(T)$ data of the following table to the above equation.

	ΔE_Q [mm s^{-1}]		Tetragonal distortion
	298 K	77K	ε [cm^{-1}]
HS	3.18	3.38	805
HS1	2.95	3.29	689
HS2	2.37	3.07	499

5. Computational details and cartesian coordinates of located stationary points

Quantum chemical calculations were performed with the Gaussian 16 program package.[6] Geometry optimizations were started from the determined X-RAY structure of **Fe-w5**, by only keeping those water molecules that were directly coordinated to iron (called Form **A** in the paper). In the case of the methanol containing-system water molecules were replaced by methanol molecules (denoted Form **B**). In order to best mimick the coordination

sphere of iron in the LS polymeric form, the water molecules were replaced by neutral tetrazole units (denoted Form **C**). Geometries were optimized with the B3LYP and the long-range corrected CAM-B3LYP functionals using the 6-31G* basis set on all atom with the exception of iron on which the SDD pseudopotential in conjunction with the corresponding basis set. This basis set combination is denoted BS1. Grimme's D3 dispersion correction[7] with the BJ-damping[8] was used in all calculations. Second derivative calculations were performed in order to ensure that the located stationary points are minima on the potential energy surface. We have also studied complexes with a mixed equatorial ligand sphere by gradually replacing the methanol molecules with tetrazole ligands. The geometry of these systems was only optimized at the B3LYP/BS1+ D3 (disp) level of theory. The calculations yielded a high-spin ground state for Form **A** and **B**, and a low-spin ground state for Form **C** in good agreement with the experiments. TD-DFT calculations were performed with both functionals using the same basis set combination as used for geometry optimizations. CAM-B3LYP clearly outperformed B3LYP by producing better agreement with experiment for the UV-VIS transitions, therefore only results obtained with it are discussed. Excitations to the 50 lowest lying states were determined. In order to obtain a qualitative representation of the electronic excitations comparable to experiment natural transition orbitals (NTOs)[9] were generated with the Gaussian 16 program package by transforming the ordinary orbital representation into a more compact form in which each excited state is expressed as a single pair of orbitals (if possible): the NTO transition occurs from excited *particle* (occupied) to the empty *hole* (unoccupied).

Table S4. Bond lengths (Å) around Fe^{II} center in the ground state of forms **A**, **B** and **C** calculated at the CAM-B3LYP/BS1 level.

Form **A**		Form **B**		Form **C**	
Fe-N1	2.100	Fe-N1	2.101	Fe-N1	1.994
Fe-N2	2.100	Fe-N2	2.101	Fe-N2	1.995
Fe-O1	2.258	Fe-O1	2.234	Fe-N3 (tetrazole)	1.991
Fe-O2	2.191	Fe-O2	2.153	Fe- N4 (tetrazole)	1.950
Fe-O3	2.191	Fe-O3	2.153	Fe- N5 (tetrazole)	1.990
Fe-O4	2.258	Fe-O4	2.234	Fe- N6 (tetrazole)	1.995

Table S5. Excitation energies (E/eV), wavelengths (λ/nm), corresponding oscillator strengths (f), and assignment of the electronic transitions of Fe^{II} HS and Fe^{II} LS complexes calculated at the cam-B3LYP/BS1 level. Natural transition orbitals (NTOs) are shown for each electronic transition and molecular orbitals are identified according to a coordinate system where axes x and y are directed towards the equatorial ligands (water in form **A**, methanol in form **B** or tetrazole in from **C**), and axis z is towards the 1,2,4-triazole-containing ligand.

E (eV)	λ (nm)	f	Contributions	Assignment
Form A (HS)				

1.4741	841.07	0.0000	85β →103β (0.14422) 85β →105β (-0.57481) 85β →106β (-0.36786) 85β →107β (0.70323) 85β →109β (-0.19690) 85β ←105β (-0.10850) 85β ←107β (0.14468)	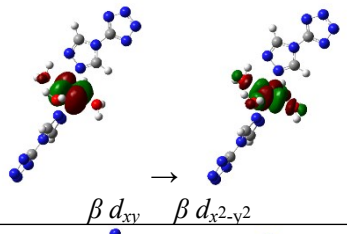 $\beta\ d_{xy}$ → $\beta\ d_{x^2-y^2}$
1.7672	701.57	0.0000	85β → 96β (-0.11889) 85β → 98β (0.31675) 85β → 99β (-0.16073) 85β →101β (-0.89335) 85β →102β (-0.14155) 85β →108β (-0.16953)	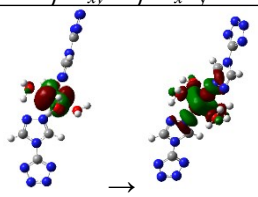 $\beta\ d_{xy}$ → $\beta\ d_{z^2}$
Form B (HS)				
1.5385	805.86	0.0000	101β →116β (0.10219) 101β →121β (-0.29175) 101β →122β (-0.94670) 101β ←122β (-0.18401)	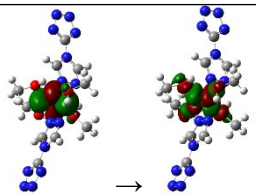 $\beta\ d_{xy}$ → $\beta\ d_{x^2-y^2}$
1.7873	693.71	0.0000	101β →114β (0.20281) 101β →115β (0.76646) 101β →117β (-0.52402) 101β →124β (-0.26681)	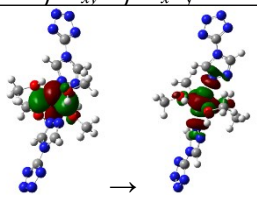 $\beta\ d_{xy}$ → $\beta\ d_{z^2}$
Form C (LS)				
2.3822	520.45	0.0000	123 →154 (0.14752) 137 →154 (0.66954)	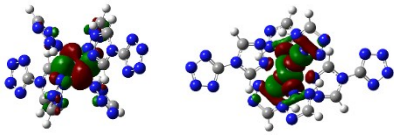 d_{xy} → $d_{x^2-y^2}$
2.4065	515.20	0.0000	135 →154 (0.20264) 135 →160 (0.16435) 136 →154 (-0.11752) 139 →154 (0.43229) 139 →160 (0.35137) 139 →161 (-0.13937)	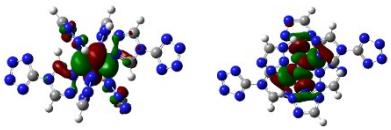 d_{xz} → $d_{x^2-y^2}$
2.4836	499.22	0.0000	122 →154 (0.10208) 135 →154 (0.11480) 136 →154 (0.19859) 136 →160 (-0.16484) 138 →154 (0.42842) 138 →160 (-0.35707) 138 →161 (0.14027)	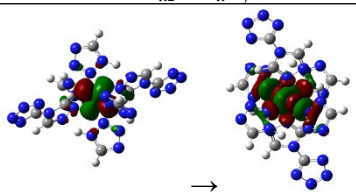 d_{yz} → $d_{x^2-y^2}$

3.4030	364.34	0.0002	135 →154 (0.17645) 135 →160 (-0.17701) 136 →154 (-0.10522) 136 →160 (0.10546) 139 →154 (0.39600) 139 →160 (-0.38980) 139 →161 (0.15216)	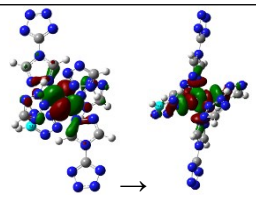 d_{xz} → d_{z^2}
3.4794	356.34	0.0002	135 →154 (0.10445) 135 →160 (0.10195) 136 →154 (0.17967) 136 →160 (0.17563) 138 →154 (0.40505) 138 →160 (0.38918) 138 →161 (-0.15268)	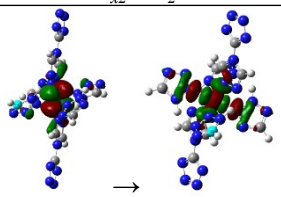 d_{yz} → d_{z^2}
3.8467	322.32	0.0000	123 →160 (0.12334) 137 →156 (0.11443) 137 →159 (-0.13558) 137 →160 (0.60014) 137 →161 (-0.23412)	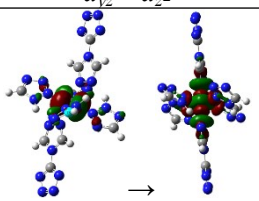 d_{xy} → d_{z^2}

CAM-B3LYP optimized geometries for which TD-DFT data was calculated

Form A (equatorial ligands: 4 water molecules) HS

opt: CAM-B3LYP/BS1 + Grimme's dispersion

-1426.53482082

0 5

26	0	-0.000004	-0.000048	-0.011875
8	0	0.434864	1.626157	-1.383097
1	0	-0.115031	1.843337	-2.151682
1	0	0.400492	2.384940	-0.772068
8	0	0.065441	1.830943	1.270439
1	0	0.580570	1.843019	2.090692
1	0	-0.901238	1.916150	1.503657
8	0	-0.065523	-1.830361	1.271063
1	0	0.901151	-1.915579	1.504284
1	0	-0.580592	-1.841928	2.091362
8	0	-0.434778	-1.626555	-1.382705
1	0	0.115034	-1.843767	-2.151340
1	0	-0.400482	-2.385377	-0.771737
7	0	-2.063401	0.338997	0.191861
7	0	-2.499264	1.298354	1.068943
6	0	-3.807517	1.276737	1.031730
1	0	-4.490502	1.896503	1.591998
7	0	-4.229828	0.329612	0.155909
6	0	-3.121268	-0.234094	-0.349989
1	0	-3.136001	-1.026420	-1.081726
6	0	-5.563487	-0.007407	-0.164444

7	0	-6.598056	0.601422	0.380921
7	0	-7.631891	-0.026704	-0.198733
7	0	-7.192938	-0.944819	-1.029837
7	0	-5.851944	-0.959128	-1.031733
7	0	2.063401	-0.338949	0.192007
7	0	2.499250	-1.298047	1.069375
6	0	3.807503	-1.276459	1.032161
1	0	4.490479	-1.896075	1.592606
7	0	4.229826	-0.329580	0.156078
6	0	3.121274	0.233991	-0.349991
1	0	3.136013	1.026107	-1.081955
6	0	5.563492	0.007341	-0.164352
7	0	6.598048	-0.601360	0.381179
7	0	7.631896	0.026607	-0.198624
7	0	7.192962	0.944508	-1.029974
7	0	5.851967	0.958830	-1.031888

Form B (equatorial ligands: 4 methanol) HS
opt: CAM-B3LYP/BS1 + Grimme's dispersion
-1583.66463840
0 5

7	0	-5.838673	-1.054906	0.946346
6	0	-5.558574	-0.191737	-0.011769
7	0	-6.598621	0.340257	-0.623029
7	0	-7.626952	-0.244254	0.010328
7	0	-7.179903	-1.065040	0.933447
7	0	-4.227746	0.137631	-0.351147
6	0	-3.810390	1.010611	-1.303447
7	0	-2.502004	1.057945	-1.323921
7	0	-2.061990	0.190450	-0.358672
6	0	-3.115064	-0.356193	0.216829
26	0	-0.000004	0.004173	0.000004
7	0	2.061985	0.190661	0.358558
7	0	2.502023	1.058682	1.323328
6	0	3.810408	1.011326	1.302849
7	0	4.227742	0.137823	0.351022
6	0	3.115045	-0.356302	-0.216663
6	0	5.558560	-0.191743	0.011801
7	0	6.598623	0.340569	0.622759
7	0	7.626938	-0.244249	-0.010339
7	0	7.179866	-1.065584	-0.932959
7	0	5.838635	-1.055454	-0.945832
8	0	-0.382249	-1.343264	1.635527
8	0	-0.097743	1.327950	1.796870

8	0	0.097779	1.326891	-1.797494
8	0	0.382239	-1.344211	-1.634734
6	0	0.414513	-2.477521	2.004528
1	0	-0.401693	-0.689094	2.356988
6	0	-0.871386	2.527520	1.877364
1	0	0.867836	1.521406	1.917744
1	0	-0.867788	1.520315	-1.918515
6	0	0.871469	2.526393	-1.878537
6	0	-0.414546	-2.478660	-2.003096
1	0	0.401696	-0.690442	-2.356556
1	0	4.496658	1.563156	1.926470
1	0	3.123591	-1.083499	-1.013173
1	0	-4.496623	1.562105	-1.927382
1	0	-3.123628	-1.082956	1.013736
1	0	-0.005903	-2.957975	2.890394
1	0	0.377327	-3.173457	1.167233
1	0	1.451742	-2.183636	2.186567
1	0	-0.799540	2.957040	2.879519
1	0	-0.536104	3.260553	1.137000
1	0	-1.907743	2.259804	1.673579
1	0	0.799704	2.955416	-2.880910
1	0	0.536166	3.259808	-1.138561
1	0	1.907803	2.258741	-1.674550
1	0	0.005867	-2.959627	-2.888685
1	0	-0.377382	-3.174120	-1.165405
1	0	-1.451766	-2.184855	-2.185311

Form C equatorial ligands: 4 tetrazole molecules LS
opt: CAM-B3LYP/BS1 + Grimme's dispersion
-2153.58202161
0 1

6	0	-0.487470	-3.035002	-2.690960
7	0	-1.376680	-2.193435	-3.184636
7	0	-1.330651	-1.114277	-2.406793
7	0	-0.453149	-1.273649	-1.467519
7	0	0.090254	-2.473119	-1.626931
26	0	-0.004501	0.000639	0.000692
7	0	-1.922464	0.525518	0.141755
7	0	-2.303632	1.842604	0.185831
6	0	-3.615602	1.854000	0.202470
7	0	-4.089321	0.587445	0.166789
6	0	-3.010755	-0.216733	0.131290
6	0	-5.444358	0.187674	0.172719
7	0	-6.432147	1.059532	0.233667

7	0	-7.511797	0.263200	0.219995
7	0	-7.141842	-0.995647	0.155520
7	0	-5.803333	-1.080399	0.123133
7	0	1.912876	-0.527791	-0.139259
7	0	2.295830	-1.844074	-0.191109
6	0	3.607835	-1.852538	-0.206333
7	0	4.079693	-0.584988	-0.160590
6	0	2.999388	0.215931	-0.121360
6	0	5.430927	-0.172889	-0.157496
7	0	6.430512	-1.032503	-0.178014
7	0	7.499841	-0.221567	-0.167976
7	0	7.113033	1.033250	-0.143241
7	0	5.772985	1.101089	-0.135833
1	0	4.256341	-2.713866	-0.251165
1	0	3.054615	1.292176	-0.088164
1	0	-4.263377	2.716141	0.241473
1	0	-3.068685	-1.293659	0.103667
1	0	-0.255449	-4.016563	-3.073439
1	0	0.915879	-2.690156	-1.031278
7	0	-0.217270	-1.458935	1.338140
7	0	-0.969617	-2.503956	1.246705
7	0	0.520112	-1.586838	2.441245
1	0	1.168589	-0.833933	2.694960
6	0	0.183378	-2.745639	3.012786
1	0	0.607800	-3.127662	3.928189
7	0	-0.743216	-3.324865	2.275568
7	0	0.437415	1.279159	1.466900
7	0	1.304977	1.128979	2.416618
7	0	-0.119243	2.473356	1.617699
1	0	-0.951743	2.670903	1.016986
7	0	1.330278	2.208776	3.195362
6	0	0.438234	3.040382	2.690254
1	0	0.189332	4.018350	3.071440
7	0	0.231417	1.453796	-1.335197
7	0	1.047454	2.467853	-1.277576
6	0	0.788683	3.192836	-2.381107
1	0	1.307198	4.103284	-2.636591
7	0	-0.171269	2.655579	-3.122373
7	0	-0.482659	1.588781	-2.431702
1	0	-1.173735	0.880121	-2.700879

Form A (equatorial ligands: 4 water molecules) HS
opt: B3LYP/BS1 + Grimme's dispersion
-1427.16131095

0 5

26	0	-0.000113	-0.000179	-0.030556
8	0	0.427604	1.635633	-1.424879
1	0	-0.175387	1.845463	-2.156813
1	0	0.401947	2.391460	-0.807495
8	0	0.079955	1.853331	1.255824
1	0	0.592190	1.839998	2.079533
1	0	-0.888323	1.926569	1.494011
8	0	-0.080037	-1.852602	1.256774
1	0	0.888274	-1.925827	1.494721
1	0	-0.592018	-1.838303	2.080626
8	0	-0.426930	-1.636102	-1.424761
1	0	0.176481	-1.845574	-2.156448
1	0	-0.401493	-2.392146	-0.807643
7	0	-2.061765	0.342244	0.176107
7	0	-2.493837	1.300493	1.068899
6	0	-3.808985	1.275473	1.042143
1	0	-4.488701	1.889808	1.612006
7	0	-4.241498	0.327274	0.158677
6	0	-3.128833	-0.233798	-0.363430
1	0	-3.146935	-1.021179	-1.099820
6	0	-5.576723	-0.006675	-0.148512
7	0	-6.611683	0.604557	0.417155
7	0	-7.659462	-0.020919	-0.155798
7	0	-7.227600	-0.943954	-1.006649
7	0	-5.879841	-0.959392	-1.024310
7	0	2.061687	-0.341844	0.176396
7	0	2.493710	-1.300099	1.069217
6	0	3.808848	-1.275268	1.042356
1	0	4.488548	-1.889598	1.612243
7	0	4.241428	-0.327109	0.158850
6	0	3.128803	0.233963	-0.363319
1	0	3.146931	1.021197	-1.099859
6	0	5.576669	0.006630	-0.148447
7	0	6.611599	-0.604485	0.417443
7	0	7.659426	0.020638	-0.155743
7	0	7.227649	0.943416	-1.006949
7	0	5.879902	0.959001	-1.024580

Form B (equatorial ligands: 4 methanol) HS
opt: B3LYP/BS1 + Grimme's dispersion
-1584.40252484
0 5

7	0	5.877123	1.003676	0.943343

6	0	5.571952	0.136263	-0.016521
7	0	6.605726	-0.434704	-0.624649
7	0	7.654923	0.125703	0.010531
7	0	7.225030	0.974637	0.935777
7	0	4.235495	-0.157613	-0.358061
6	0	3.796474	-1.033359	-1.310769
7	0	2.480657	-1.048029	-1.338885
7	0	2.056184	-0.155021	-0.378642
6	0	3.125346	0.372900	0.201909
26	0	-0.000005	0.051061	0.000002
7	0	-2.056192	-0.155146	0.378584
7	0	-2.480671	-1.048471	1.338531
6	0	-3.796488	-1.033777	1.310422
7	0	-4.235504	-0.157722	0.357996
6	0	-3.125351	0.372968	-0.201797
6	0	-5.571959	0.136266	0.016543
7	0	-6.605737	-0.434914	0.624465
7	0	-7.654931	0.125760	-0.010486
7	0	-7.225031	0.974957	-0.935487
7	0	-5.877123	1.003972	-0.943057
8	0	0.394989	1.416715	1.635717
8	0	0.131975	-1.273270	1.817349
8	0	-0.132004	-1.272672	-1.817705
8	0	-0.394956	1.417262	-1.635260
6	0	-0.458313	2.520691	1.999902
1	0	0.423714	0.760583	2.357541
6	0	0.919734	-2.473626	1.856741
1	0	-0.832814	-1.483763	1.932066
1	0	0.832780	-1.483126	-1.932528
6	0	-0.919755	-2.473025	-1.857392
6	0	0.458410	2.521293	-1.999131
1	0	-0.423778	0.761375	-2.357301
1	0	-4.472146	-1.608208	1.924914
1	0	-3.146705	1.106291	-0.991865
1	0	4.472128	-1.607597	-1.925447
1	0	3.146702	1.105965	0.992215
1	0	-0.067358	3.016796	2.892041
1	0	-0.439477	3.216883	1.161006
1	0	-1.484795	2.181211	2.168851
1	0	0.848067	-2.940604	2.843390
1	0	0.593999	-3.181834	1.086773
1	0	1.953827	-2.185554	1.665815
1	0	-0.848147	-2.939719	-2.844180
1	0	-0.593965	-3.181449	-1.087647

1	0	-1.953839	-2.185015	-1.666318
1	0	0.067435	3.017727	-2.891077
1	0	0.439687	3.217204	-1.160001
1	0	1.484853	2.181786	-2.168263

equatorial ligands: 1 methanol + 3 tetrazol HS
opt: B3LYP/BS1 + Grimme's dispersion
-2012.02516439
0 5

6	0	-0.925590	-4.039363	0.631188
7	0	-0.862867	-3.980713	-0.693202
7	0	-0.594126	-2.701475	-0.991073
7	0	-0.490498	-1.991054	0.093945
7	0	-0.696803	-2.813930	1.128368
26	0	0.038214	0.162498	0.028427
7	0	-2.042233	0.574643	-0.359293
7	0	-2.467641	1.596556	-1.183188
6	0	-3.764735	1.431937	-1.358038
7	0	-4.191021	0.332590	-0.675930
6	0	-3.094633	-0.174501	-0.067979
6	0	-5.500266	-0.186389	-0.602984
7	0	-6.531704	0.383252	-1.214834
7	0	-7.550262	-0.433051	-0.874304
7	0	-7.105407	-1.417470	-0.103780
7	0	-5.777657	-1.285723	0.090861
8	0	0.285584	-0.263064	-2.104335
7	0	2.086165	-0.156967	0.204584
7	0	2.715792	-0.343938	1.418240
6	0	3.988929	-0.514210	1.141612
7	0	4.205276	-0.442673	-0.209414
6	0	2.996285	-0.222334	-0.762237
6	0	5.433663	-0.562450	-0.892189
7	0	6.581795	-0.788233	-0.262915
7	0	7.465640	-0.820301	-1.281842
7	0	6.838022	-0.620160	-2.433180
7	0	5.518022	-0.448720	-2.214224
1	0	-0.034191	-1.180993	-2.230616
6	0	-0.014084	0.545202	-3.253937
1	0	4.790094	-0.689962	1.842446
1	0	2.832272	-0.132093	-1.822355
1	0	-4.430860	2.047757	-1.942349
1	0	-3.128151	-1.058024	0.547909
1	0	-1.129238	-4.918343	1.223116

1	0	-0.631876	-2.405929	2.074628
1	0	0.400440	0.083066	-4.154066
1	0	-1.092804	0.691278	-3.360165
1	0	0.471806	1.509008	-3.092315
7	0	0.005193	0.230014	2.277595
7	0	-0.198014	-0.795742	3.054768
7	0	0.705378	1.117092	2.989160
1	0	1.066150	1.953955	2.510636
6	0	0.928743	0.592594	4.200474
1	0	1.480211	1.077085	4.991043
7	0	0.356325	-0.602145	4.258936
7	0	0.261296	2.401185	0.094911
7	0	1.028317	3.080519	0.898928
7	0	-0.425208	3.282643	-0.639798
1	0	-1.242681	2.885978	-1.165723
7	0	0.859000	4.399678	0.709522
6	0	-0.054334	4.511592	-0.245223
1	0	-0.442745	5.433162	-0.650645

equatorial ligands: 2 methanol + 2 tetrazol HS
opt: B3LYP/BS1 + Grimme's dispersion
-1869.48665169
0 5

6	0	2.340736	-3.124940	0.581123
7	0	1.887567	-3.056209	1.828466
7	0	0.887413	-2.156006	1.812629
7	0	0.710329	-1.685163	0.613518
7	0	1.609665	-2.291542	-0.175900
26	0	-0.102225	0.381198	0.298307
7	0	1.976610	1.126762	0.556844
7	0	2.457592	2.047413	-0.359803
6	0	3.676854	1.672730	-0.683558
7	0	4.009975	0.533705	-0.006174
6	0	2.944320	0.251459	0.776452
6	0	5.080376	-0.357797	-0.248644
7	0	6.262409	0.003200	-0.723848
7	0	6.891878	-1.184430	-0.869652
7	0	6.093655	-2.171296	-0.496517
7	0	4.905501	-1.673046	-0.097922
8	0	-0.522144	0.252168	2.378858
7	0	-1.995178	-0.290892	-0.317426
7	0	-2.077300	-0.987384	-1.502437
6	0	-3.332819	-1.358103	-1.637394
7	0	-4.064028	-0.919950	-0.571319

6	0	-3.199626	-0.256717	0.230936
6	0	-5.442761	-1.122538	-0.351032
7	0	-6.211072	-1.768306	-1.222081
7	0	-7.417345	-1.731731	-0.620845
7	0	-7.326936	-1.092204	0.538646
7	0	-6.057741	-0.685094	0.742638
1	0	-0.175171	-0.601682	2.711230
6	0	-0.388968	1.291126	3.367255
1	0	-3.769040	-1.920914	-2.447683
1	0	-3.485840	0.219164	1.154571
1	0	4.343328	2.153973	-1.383022
1	0	2.924961	-0.584745	1.454927
1	0	3.181499	-3.699594	0.227795
1	0	1.686973	-1.987919	-1.143173
1	0	-0.840040	0.966113	4.308091
1	0	0.664007	1.550275	3.517491
1	0	-0.933541	2.153648	2.983632
7	0	-0.688106	2.472123	0.089317
7	0	-1.865183	2.975762	0.326168
7	0	0.115816	3.478083	-0.295492
1	0	1.114472	3.244976	-0.480021
7	0	-1.851442	4.300977	0.105742
6	0	-0.615667	4.599639	-0.276140
1	0	-0.246971	5.580670	-0.533491
8	0	0.421110	-0.236239	-1.819378
1	0	-0.452704	-0.708516	-1.976353
6	0	0.573190	0.730776	-2.875441
1	0	-0.302716	1.386987	-2.923124
1	0	1.461011	1.320474	-2.650996
1	0	0.703518	0.221300	-3.834894

equatorial ligands: 3 methanol + 1 tetrazol HS
opt: B3LYP/BS1 + Grimme's dispersion
-1726.94542261
0 5

6	0	-0.778655	3.944137	-0.491041
7	0	-0.611936	4.014608	0.820333
7	0	-0.331063	2.760811	1.224834
7	0	-0.321169	1.948799	0.213435
7	0	-0.600804	2.667185	-0.877491
26	0	0.073640	-0.240876	0.255280
7	0	-1.992002	-0.702755	0.336485
7	0	-2.374574	-2.028129	0.326128
6	0	-3.684546	-2.044201	0.196147

7	0	-4.163323	-0.766659	0.118826
6	0	-3.082400	0.039733	0.213570
6	0	-5.497133	-0.347531	-0.067252
7	0	-6.518481	-1.194096	-0.118749
7	0	-7.563907	-0.367040	-0.328340
7	0	-7.143415	0.889419	-0.393068
7	0	-5.805528	0.935854	-0.229701
8	0	-0.148727	0.115818	-1.953735
8	0	0.261493	-2.350454	0.420895
8	0	0.411066	0.221671	2.310232
7	0	2.139161	-0.047236	-0.264884
7	0	2.443517	0.054411	-1.603934
6	0	3.758711	0.061508	-1.699235
7	0	4.312643	-0.033096	-0.458625
6	0	3.274226	-0.098484	0.411714
6	0	5.686144	-0.070451	-0.137520
7	0	6.635265	0.012253	-1.063145
7	0	7.761337	-0.072847	-0.325021
7	0	7.453707	-0.198417	0.959207
7	0	6.113652	-0.201235	1.113899
6	0	-0.862491	-0.822208	-2.781901
1	0	0.833980	0.099465	-2.174559
1	0	-0.671307	-2.685653	0.397188
6	0	1.193645	-3.276880	-0.154022
1	0	0.245264	1.177033	2.455139
6	0	-0.216848	-0.560463	3.351685
1	0	4.352428	0.128668	-2.597441
1	0	3.398826	-0.177562	1.479905
1	0	-4.328047	-2.908981	0.148783
1	0	-3.152366	1.115063	0.187662
1	0	-1.021507	4.762628	-1.151064
1	0	-0.618772	2.169050	-1.767042
1	0	-0.758849	-0.546183	-3.835101
1	0	-0.488214	-1.839102	-2.627070
1	0	-1.912607	-0.777050	-2.492961
1	0	1.171916	-4.221170	0.397334
1	0	0.966591	-3.458168	-1.210488
1	0	2.183442	-2.829350	-0.067904
1	0	0.204787	-0.282234	4.320421
1	0	-1.300497	-0.411641	3.345353
1	0	0.014153	-1.602066	3.131234

Form C (equatorial ligands: 0 methanol + 4 tetrazol HS
opt: B3LYP/BS1 + Grimme's dispersion

-2154.5739318

0 5

6	0	-0.427627	-3.824043	-2.048918
7	0	-0.357660	-3.032528	-3.112031
7	0	-0.350462	-1.783692	-2.629212
7	0	-0.413345	-1.785321	-1.327923
7	0	-0.466997	-3.062612	-0.947450
26	0	-0.001669	-0.000024	-0.004419
7	0	-2.009990	0.522250	0.033313
7	0	-2.379251	1.850353	0.061558
6	0	-3.694050	1.858273	0.059482
7	0	-4.186593	0.579584	0.031573
6	0	-3.106402	-0.226679	0.016208
6	0	-5.535528	0.168504	0.016517
7	0	-6.549058	1.026647	0.038318
7	0	-7.619655	0.205771	0.010468
7	0	-7.221313	-1.058989	-0.025463
7	0	-5.873725	-1.117056	-0.022806
7	0	2.006921	-0.522292	-0.042301
7	0	2.377180	-1.850131	-0.070368
6	0	3.692019	-1.857120	-0.059649
7	0	4.183494	-0.578251	-0.025762
6	0	3.102763	0.227349	-0.016136
6	0	5.532095	-0.166677	-0.001070
7	0	6.545975	-1.024548	-0.017140
7	0	7.616161	-0.203451	0.019135
7	0	7.217237	1.061152	0.054104
7	0	5.869708	1.118900	0.042351
1	0	4.338539	-2.720710	-0.074158
1	0	3.170305	1.302978	0.007911
1	0	-4.339947	2.722280	0.076896
1	0	-3.175241	-1.302329	-0.005709
1	0	-0.454461	-4.902604	-2.055735
1	0	-0.472955	-3.258647	0.070043
7	0	-0.251827	-1.328983	1.813814
7	0	-0.455720	-2.613940	1.827179
7	0	-0.080473	-0.951870	3.083646
1	0	0.106391	0.053315	3.264206
6	0	-0.186720	-2.044530	3.854920
1	0	-0.093840	-2.053101	4.929949
7	0	-0.422378	-3.093356	3.078498
7	0	0.410210	1.783841	1.321095
7	0	0.357651	1.782668	2.622891
7	0	0.455985	3.060872	0.939547

1	0	0.454245	3.257885	-0.077529
7	0	0.364733	3.031763	3.104976
6	0	0.422925	3.822881	2.040858
1	0	0.446403	4.901521	2.046821
7	0	0.251475	1.329111	-1.822095
7	0	0.447573	2.615489	-1.835076
7	0	0.099854	0.948830	-3.093453
1	0	-0.079108	-0.057292	-3.275017
6	0	0.209514	2.040783	-3.865331
1	0	0.131541	2.047050	-4.941521
7	0	0.428233	3.092335	-3.087465

Form A (equatorial ligands: 4 water molecules) LS
opt: B3LYP/BS1 + Grimme's dispersion
-1427.1359045
0 1

26	0	-0.000033	-0.175225	-0.000004
8	0	0.217546	1.251315	1.463902
1	0	-0.610220	1.749611	1.583875
1	0	0.335599	0.731509	2.281042
8	0	0.089096	-1.504522	1.551002
1	0	0.672544	-2.270839	1.427292
1	0	-0.861644	-1.815347	1.605355
8	0	-0.088812	-1.501522	-1.553443
1	0	0.861704	-1.813165	-1.607586
1	0	-0.673121	-2.267451	-1.431516
8	0	-0.218507	1.253934	-1.460999
1	0	0.607067	1.756806	-1.576913
1	0	-0.331846	0.736124	-2.280086
7	0	-1.967802	-0.265825	0.250074
7	0	-2.455246	-1.309838	1.006195
6	0	-3.769806	-1.206188	0.992238
1	0	-4.483354	-1.851211	1.480961
7	0	-4.143992	-0.128408	0.247449
6	0	-2.997125	0.436530	-0.201343
1	0	-2.973302	1.313780	-0.827959
6	0	-5.455642	0.319826	-0.014077
7	0	-6.529276	-0.298567	0.463914
7	0	-7.533742	0.456052	-0.026864
7	0	-7.041036	1.454319	-0.748963
7	0	-5.693997	1.393578	-0.760081
7	0	1.967870	-0.265499	-0.250103
7	0	2.455198	-1.309053	-1.006912
6	0	3.769752	-1.205457	-0.993081

1	0	4.483187	-1.850236	-1.482295
7	0	4.144074	-0.128169	-0.247658
6	0	2.997249	0.436507	0.201602
1	0	2.973649	1.313394	0.828746
6	0	5.455760	0.319876	0.014030
7	0	6.529374	-0.298094	-0.464556
7	0	7.533917	0.455967	0.026853
7	0	7.041181	1.453782	0.749626
7	0	5.694176	1.392993	0.760925

Form B (equatorial ligands: 4 methanol molecules) LS opt: B3LYP/BS1 + Grimme's dispersion

-1584.37914358

0 1

7	0	5.686344	1.293691	0.892184
6	0	5.448510	0.334707	0.003057
7	0	6.522278	-0.198725	-0.567693
7	0	7.526195	0.488251	0.016434
7	0	7.033166	1.368758	0.877113
7	0	4.137054	-0.083768	-0.305947
6	0	3.758267	-1.047028	-1.192606
7	0	2.443964	-1.155171	-1.205079
7	0	1.962598	-0.233938	-0.302845
6	0	2.991961	0.403781	0.231486
26	0	-0.000000	-0.151553	-0.000070
7	0	-1.962593	-0.233974	0.302776
7	0	-2.443907	-1.155129	1.205113
6	0	-3.758212	-1.047001	1.192694
7	0	-4.137048	-0.083796	0.305994
6	0	-2.991985	0.403725	-0.231527
6	0	-5.448521	0.334671	-0.002951
7	0	-6.522255	-0.198721	0.567901
7	0	-7.526175	0.488666	-0.015736
7	0	-7.033255	1.368242	-0.877429
7	0	-5.686405	1.293603	-0.892120
8	0	0.297625	1.244073	1.492432
8	0	0.131697	-1.455191	1.590667
8	0	-0.131639	-1.455428	-1.590581
8	0	-0.297696	1.243791	-1.492761
6	0	-0.698595	2.244470	1.807416
1	0	0.416598	0.655905	2.260700
6	0	0.986526	-2.610670	1.632160
1	0	-0.827764	-1.694657	1.721296
1	0	0.827844	-1.694812	-1.721216

6	0	-0.986356	-2.610997	-1.631929
6	0	0.698444	2.244242	-1.807836
1	0	-0.416631	0.655555	-2.260993
1	0	-4.467660	-1.612287	1.776561
1	0	-2.967930	1.190497	-0.967229
1	0	4.467748	-1.612349	-1.776400
1	0	2.967864	1.190602	0.967135
1	0	-0.302376	2.916014	2.572943
1	0	-0.882185	2.798541	0.887575
1	0	-1.628018	1.779011	2.143571
1	0	0.831593	-3.143022	2.574146
1	0	0.789835	-3.277560	0.787076
1	0	2.013781	-2.252834	1.577008
1	0	-0.831346	-3.143474	-2.573831
1	0	-0.789626	-3.277741	-0.786738
1	0	-2.013640	-2.253239	-1.576859
1	0	0.302179	2.915672	-2.573440
1	0	0.881978	2.798427	-0.888053
1	0	1.627909	1.778828	-2.143934

equatorial ligands: 3 methanol + tetrazole molecules LS
opt: B3LYP/BS1 + Grimme's dispersion
-1726.92691012
0 1

6	0	-0.656054	3.658180	-0.912484
7	0	-0.540558	3.776814	0.400172
7	0	-0.291614	2.540190	0.868529
7	0	-0.253363	1.688633	-0.112671
7	0	-0.479876	2.365602	-1.244119
26	0	0.062879	-0.240877	0.009194
7	0	-1.889007	-0.624917	0.199371
7	0	-2.309056	-1.934367	0.140997
6	0	-3.626781	-1.911050	0.166769
7	0	-4.069709	-0.623364	0.235807
6	0	-2.959965	0.152303	0.259995
6	0	-5.402999	-0.162270	0.239628
7	0	-6.447249	-0.981822	0.243528
7	0	-7.485565	-0.119736	0.221845
7	0	-7.039055	1.128942	0.204802
7	0	-5.690166	1.135578	0.213465
8	0	-0.096098	-0.229553	-2.131450
8	0	0.295246	-2.277459	0.282208
8	0	0.393231	0.054655	2.044979
7	0	2.012889	-0.049975	-0.330094

7	0	2.458048	-0.156014	-1.627372
6	0	3.775527	-0.117509	-1.580482
7	0	4.189298	0.009139	-0.289041
6	0	3.063830	0.049551	0.467126
6	0	5.520078	0.071141	0.176092
7	0	6.561782	0.028240	-0.646998
7	0	7.603095	0.104116	0.207384
7	0	7.160956	0.185107	1.455449
7	0	5.812214	0.165306	1.468873
6	0	-0.865193	-1.210819	-2.852466
1	0	0.884754	-0.303708	-2.334676
1	0	-0.629442	-2.619565	0.174823
6	0	1.271277	-3.114528	-0.354398
1	0	0.185945	0.997196	2.207869
6	0	-0.274257	-0.768117	3.027400
1	0	4.464195	-0.174780	-2.408787
1	0	3.063067	0.139020	1.540751
1	0	-4.296343	-2.756386	0.135903
1	0	-3.000162	1.227305	0.324640
1	0	-0.860832	4.453224	-1.612836
1	0	-0.482127	1.831390	-2.111915
1	0	-0.703751	-1.084050	-3.926418
1	0	-0.588745	-2.223874	-2.548651
1	0	-1.913902	-1.039156	-2.612507
1	0	1.109024	-4.152967	-0.053986
1	0	1.225236	-3.028707	-1.445287
1	0	2.251097	-2.786492	-0.009338
1	0	0.095056	-0.506444	4.022008
1	0	-1.358543	-0.636983	2.972347
1	0	-0.012637	-1.796984	2.788550

equatorial ligands: 2 methanol + 2 tetrazole molecules LS
opt: B3LYP/BS1 + Grimme's dispersion
-1869.46718957
0 1

6	0	1.952864	-3.179229	-0.099022
7	0	1.475433	-3.293114	1.133571
7	0	0.626457	-2.263625	1.304709
7	0	0.569549	-1.540779	0.226373
7	0	1.382637	-2.107444	-0.675065
26	0	-0.083062	0.362199	0.145201
7	0	1.913789	0.920841	0.487580
7	0	2.508661	1.976724	-0.177340
6	0	3.782536	1.673225	-0.327239

7	0	4.036418	0.452413	0.226569
6	0	2.863152	0.040700	0.756896
6	0	5.139517	-0.413389	0.040931
7	0	6.389061	-0.020530	-0.149997
7	0	7.029810	-1.192654	-0.360025
7	0	6.172115	-2.199367	-0.293566
7	0	4.933038	-1.730948	-0.045841
8	0	-0.592408	0.150924	2.160665
7	0	-1.906364	-0.230444	-0.337778
7	0	-2.140401	-0.595714	-1.640964
6	0	-3.413751	-0.929344	-1.717539
7	0	-4.001020	-0.789844	-0.497091
6	0	-3.032919	-0.348139	0.342517
6	0	-5.346739	-1.057447	-0.165120
7	0	-6.229895	-1.471720	-1.066622
7	0	-7.351455	-1.602804	-0.327801
7	0	-7.104224	-1.275972	0.933520
7	0	-5.810735	-0.917964	1.071999
1	0	-0.304995	-0.754469	2.401161
6	0	-0.156617	1.095053	3.158947
1	0	-3.952452	-1.268336	-2.588195
1	0	-3.195118	-0.128024	1.383771
1	0	4.537524	2.266197	-0.820170
1	0	2.768372	-0.893138	1.283055
1	0	2.702466	-3.802520	-0.560636
1	0	1.494902	-1.643580	-1.573842
1	0	-0.499077	0.763023	4.141967
1	0	0.931816	1.204010	3.145877
1	0	-0.630051	2.044811	2.912394
7	0	-0.666862	2.277537	0.098204
7	0	-1.873042	2.741222	0.268950
7	0	0.153512	3.327127	-0.090250
1	0	1.170578	3.129843	-0.220773
7	0	-1.859943	4.082055	0.197973
6	0	-0.600034	4.432213	-0.024840
1	0	-0.226719	5.438379	-0.138631
8	0	0.322983	0.149399	-1.979499
1	0	-0.594451	-0.219541	-2.190862
6	0	0.561447	1.278694	-2.840708
1	0	-0.265658	1.992436	-2.773646
1	0	1.487081	1.749589	-2.512064
1	0	0.668280	0.932583	-3.872666

equatorial ligands: 1 methanol + 3 tetrazole molecules LS

opt: B3LYP/BS1 + Grimme's dispersion

-2012.01150221

0 1

6	0	-0.847770	-3.916172	-0.374370
7	0	-0.456654	-3.628591	-1.607155
7	0	-0.190345	-2.314234	-1.614249
7	0	-0.406814	-1.802064	-0.438398
7	0	-0.825071	-2.791141	0.358128
26	0	0.006916	0.153772	0.009856
7	0	-1.977726	0.652674	-0.209021
7	0	-2.405401	1.868540	-0.693530
6	0	-3.717372	1.795382	-0.817981
7	0	-4.149699	0.565726	-0.429355
6	0	-3.042791	-0.118482	-0.055964
6	0	-5.470997	0.072557	-0.414375
7	0	-6.516138	0.806908	-0.774932
7	0	-7.540159	-0.056201	-0.609454
7	0	-7.084602	-1.223849	-0.174825
7	0	-5.743919	-1.173018	-0.038528
8	0	0.364527	0.360415	-2.209888
7	0	1.923540	-0.361321	0.096529
7	0	2.341974	-1.403529	0.892624
6	0	3.640025	-1.505048	0.696214
7	0	4.068529	-0.563869	-0.198539
6	0	2.968668	0.133916	-0.554919
6	0	5.385768	-0.342887	-0.654813
7	0	6.417979	-1.064153	-0.232758
7	0	7.447992	-0.512132	-0.908972
7	0	7.009350	0.476312	-1.675704
7	0	5.674154	0.612231	-1.533099
1	0	0.568369	-0.581307	-2.388389
6	0	-0.661258	0.746929	-3.145832
1	0	4.312932	-2.213910	1.152656
1	0	2.981293	0.950075	-1.258016
1	0	-4.385761	2.565851	-1.169496
1	0	-3.082967	-1.132407	0.304101
1	0	-1.145741	-4.885084	-0.004475
1	0	-0.990374	-2.571532	1.349452
1	0	-0.269366	0.662114	-4.162950
1	0	-1.553129	0.123536	-3.031242
1	0	-0.913868	1.784857	-2.936881
7	0	-0.071393	-0.190247	1.999487
7	0	-0.674860	-1.155089	2.630945
7	0	0.736797	0.410638	2.878579

1	0	1.334061	1.181427	2.550225
6	0	0.604266	-0.223304	4.052833
1	0	1.134264	0.037104	4.955958
7	0	-0.277708	-1.201259	3.911161
7	0	0.485981	2.101971	0.358319
7	0	1.435351	2.550351	1.134381
7	0	-0.130583	3.159182	-0.179286
1	0	-1.063677	2.951279	-0.628484
7	0	1.452158	3.890185	1.118882
6	0	0.472071	4.256869	0.303584
1	0	0.195126	5.269912	0.055524

Form C equatorial ligands: 4 tetrazole molecules LS
opt: B3LYP/BS1 + Grimme's dispersion
-2154.56001329
0 1

6	0	-0.719817	-0.245742	-4.183141
7	0	-0.380206	1.026362	-4.027022
7	0	-0.163823	1.181747	-2.716793
7	0	-0.361093	0.064028	-2.075068
7	0	-0.718257	-0.842752	-2.983595
26	0	-0.001116	-0.293088	-0.010356
7	0	-1.944633	-0.303398	0.406326
7	0	-2.464568	-1.151566	1.356062
6	0	-3.761717	-0.921380	1.372529
7	0	-4.092281	0.046406	0.464858
6	0	-2.931157	0.409715	-0.121072
6	0	-5.366079	0.578702	0.172729
7	0	-6.472519	0.186694	0.792379
7	0	-7.417323	0.948669	0.199713
7	0	-6.861508	1.733203	-0.712375
7	0	-5.529808	1.517446	-0.755009
7	0	1.941730	-0.295346	-0.429384
7	0	2.433190	-0.980257	-1.516126
6	0	3.729851	-0.747928	-1.531433
7	0	4.087547	0.064517	-0.491182
6	0	2.944098	0.326191	0.177856
6	0	5.368054	0.557133	-0.161116
7	0	6.460484	0.248782	-0.849146
7	0	7.417731	0.935667	-0.188523
7	0	6.882055	1.599792	0.825501
7	0	5.551767	1.375805	0.870766
1	0	4.447464	-1.122805	-2.244243
1	0	2.907034	0.947792	1.057527

1	0	-4.498059	-1.403928	1.995871
1	0	-2.871101	1.164094	-0.888470
1	0	-0.966124	-0.733312	-5.113538
1	0	-0.839474	-1.821830	-2.650111
7	0	-0.079717	-2.365426	-0.311338
7	0	-0.551617	-2.989604	-1.351430
7	0	0.352130	-3.299558	0.535108
1	0	0.702213	-2.983221	1.461504
6	0	0.120835	-4.496845	-0.021204
1	0	0.360734	-5.444110	0.436075
7	0	-0.440535	-4.314710	-1.207629
7	0	0.403612	-0.573128	2.077991
7	0	0.791296	-1.671491	2.658503
7	0	0.179137	0.315331	3.048498
1	0	-0.071572	1.283907	2.770344
7	0	0.824443	-1.528195	3.987644
6	0	0.444966	-0.279729	4.220080
1	0	0.361670	0.196059	5.184938
7	0	0.042055	1.914330	0.324754
7	0	-0.069389	2.528634	1.467896
7	0	0.191499	2.859079	-0.605756
1	0	0.214369	2.540601	-1.594955
6	0	0.159673	4.051237	0.008367
1	0	0.250204	5.004320	-0.489500
7	0	0.002805	3.855309	1.310414

6. Magnetic dilution

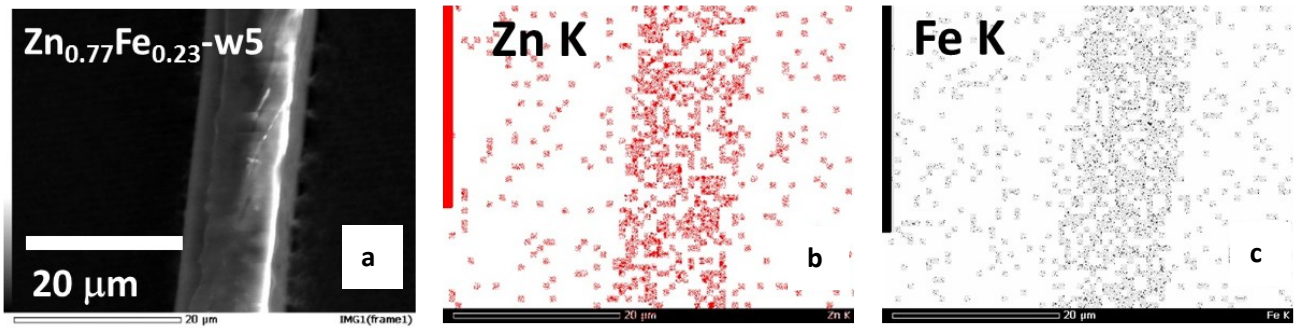

21

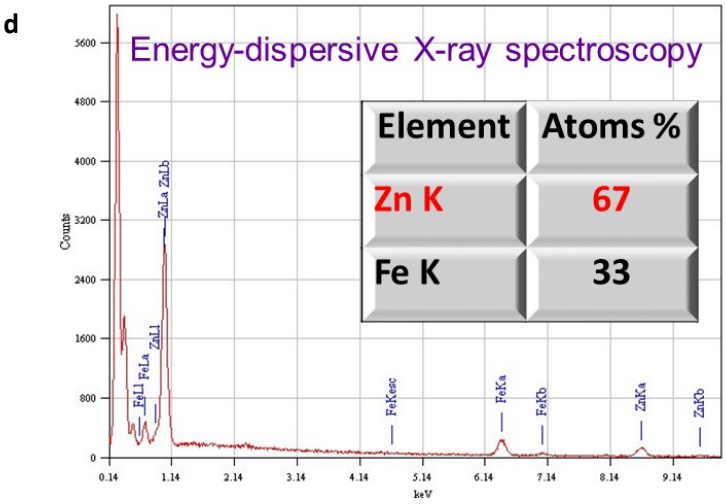

Figure S13. (a), (b) and (c) SEM image of **$Fe_{0.23}Zn_{0.77}$-w5** and the corresponding EELS elemental maps of Zn (red) and Fe (black). (d) SEM-EDX spectrum. Quantitative EDX analysis suggests Zn and Fe contents of 67 and 33 at. %, respectively. (Note: The difference between ICP and SEM-EDX results stem from the surface analysis provided by SEM-EDX).

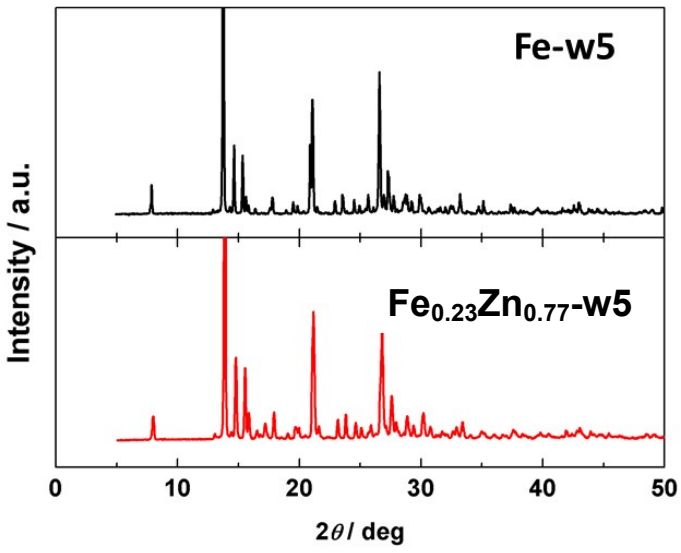

Figure S14. Room temperature powder X-ray diffraction patterns of $[Fe_xZn_{1-x}(trz\text{-}tet)_2(H_2O)_4]\cdot 5H_2O$ (**Fe_xZn_{1-x}-w5**) (x = 1 and 0.77).

References

[ ] Naik, A. D.; Robeyns, K.; Meunier, C. F.; Léonard, A. F.; Rotaru, A.; Tinant, B.; Filinchuk, Y.; Su, B. L.; Garcia, Y. Selective and reusable iron(II)-based molecular sensor for the vapor-phase detection of alcohols. *Inorg. Chem.* **2014**, *53*, 1263.

[2] Gonser, U. *Mössbauer Spectroscopy*, Springer-Verlag Berlin Heidelberg, 1975.

[3] Ingalls, R. Variational Calculation of the Sternheimer Factors for the Ferrous Ion, *Physical Rev.* **1962**, *128*, 1155-1158.

[4] Gütlich, P.; Garcia, Y. Chemical applications of Mössbauer spectroscopy in 'Mössbauer spectroscopy – Tutorial Book' (Eds Yoshida, Y.; Langouche, G.) Springer, 2013, chapter 2, 23-89.

[5] Edwards, P. R.; Jonhson, C. E.; Williams, R. J. P. Mössbauer Spectra of Some Tetrahedral Iron(II) Compounds, *J. Chem. Phys*. **1967**, *47*, 2074-2082.

[6] Gaussian 16, Revision C.01, Frisch, M. J.; Trucks, G. W.; Schlegel, H. B.; Scuseria, G. E.; Robb, M. A.; Cheeseman, J. R.; Scalmani, G.; Barone, V.; Petersson, G. A.; Nakatsuji, H.; Li, X.; Caricato, M.; Marenich, A. V.; Bloino, J.; Janesko, B. G.; Gomperts, R.; Mennucci, B.; Hratchian, H. P.; Ortiz, J. V.; Izmaylov, A. F.; Sonnenberg, J. L.; Williams-Young, D.; Ding, F.; Lipparini, F.; Egidi, F.; Goings, J.; Peng, B.; Petrone, A.; Henderson, T.; Ranasinghe, D.; Zakrzewski, V. G.; Gao, J.; Rega, N.; Zheng, G.; Liang, W.; Hada, M.; Ehara, M.; Toyota, K.; Fukuda, R.; Hasegawa, J.; Ishida, M.; Nakajima, T.; Honda, Y.; Kitao, O.; Nakai, H.; Vreven, T.; Throssell, K.; Montgomery, J. A., Jr.; Peralta, J. E.; Ogliaro, F.; Bearpark, M. J.; Heyd, J. J.; Brothers, E. N.; Kudin, K. N.; Staroverov, V. N.; Keith, T. A.; Kobayashi, R.; Normand, J.; Raghavachari, K.; Rendell, A. P.; Burant, J. C.; Iyengar, S. S.; Tomasi, J.; Cossi, M.; Millam, J. M.; Klene, M.; Adamo, C.; Cammi, R.; Ochterski, J. W.; Martin, R. L.; Morokuma, K.; Farkas, O.; Foresman, J. B.; Fox, D. J. Gaussian, Inc., Wallingford CT, 2016.

[7] Grimme, S.; Antony, J.; Ehrlich, S.; Krieg, H. A consistent and accurate ab initio parametrization of density functional dispersion correction (DFT-D) for the 94 elements H-Pu *J. Chem. Phys.* **2010**, *132*, 154104.

[8] Grimme, S.; Ehrlich, S.; Goerigk, L. Effect of the damping function in dispersion corrected density functional theory. *J. Comput. Chem.* **2011**, *32*, 1456-1365.

[9] Martin, R. L. Natural transition orbitals. *J. Chem. Phys*. **2003**, *118*, 4775-77.